

Off-axis emission from relativistic plasma flows

E.V. Derishev¹, F.A. Aharonian², Vl.V. Kocharovsky¹

¹ *Institute of Applied Physics, 46 Ulyanov st., 603950 Nizhny Novgorod, Russia*

² *Max-Planck-Institut für Kernphysik, Saupfercheckweg 1, D-69117 Heidelberg, Germany*

ABSTRACT

We show that there is no universal law describing how the spectra and luminosity of synchrotron and inverse Compton radiation from relativistic jets change with increasing observation angle. Instead, the physics of particle acceleration leaves pronounced imprints in the observed spectra and allows for a freedom in numerous modifications of them. The impact of these effects is the largest for high-energy radiation and depends on the details of particle acceleration mechanism(s), what can be used to discriminate between different models. Generally, the beam patterns of relativistic jets in GeV-TeV spectral domain are much wider than the inverse Lorentz factor. The off-axis emission in this energy range appear to be brighter, have much harder spectra and a much higher cut-off frequency compared to the values derived from Doppler boosting considerations alone.

The implications include the possibility to explain high-latitude unidentified EGRET sources as off-axis but otherwise typical relativistic-jet sources, such as blazars, and the prediction of GeV-TeV afterglow from transient jet sources, such as Gamma-Ray Bursts. We also discuss the phenomenon of beam-pattern broadening in application to neutrino emission.

Subject headings: gamma rays: bursts — gamma rays: theory — ISM: jets and outflows — neutrinos — radiation mechanisms: non-thermal — shock waves

1. Introduction

Fast-moving plasma outflows are core elements in models of bright and rapidly variable astrophysical sources, such as Active Galactic Nuclei (AGNs), Gamma-Ray Bursts (GRBs), and microquasars (see, for example, Urry & Padovani 1995 for a review on AGNs, Zhang & Mészáros 2004; Piran 2005 for reviews on GRBs). Relativistic flows offer a simple solution to the gamma-ray transparency problem for compact objects: thanks to the Lorentz boosting, variability timescales – as seen in the lab frame – decrease, the energies of individual photons

and bolometric brightness increase, whereas the pair-production opacity can be made smaller than unity for a source of any size.

Relativistic flows can be formed by hot plasma left behind a relativistic shock or exist in the form of jets. In either case the question about properties of emission from these flows naturally divides into two. Firstly, one has to know the distribution of radiating particles in the plasma comoving frame – a problem far from complete solution as it depends on details of the acceleration mechanism. Secondly, the resulting photon field needs to be recalculated for the lab frame, i.e., Lorentz-transformed from the comoving frame. This is regarded as a routine and obvious procedure and usually receives little attention.

So far, all calculations were made under silent assumption that the radiation is isotropic in the comoving frame. In many situations the aforementioned isotropy is a good guess, as is discussed in more detail in the following section. In this paper, however, we would like to emphasize that this assumption is model-dependent, and that highly relativistic jets and shock waves violate it in many situations. Abandoning the isotropy assumption has a profound effect on the predicted spectra and timing of the astrophysical sources with relativistic plasma flows (hereafter we will call them jets for short, that does not mean we exclude shocks from consideration).

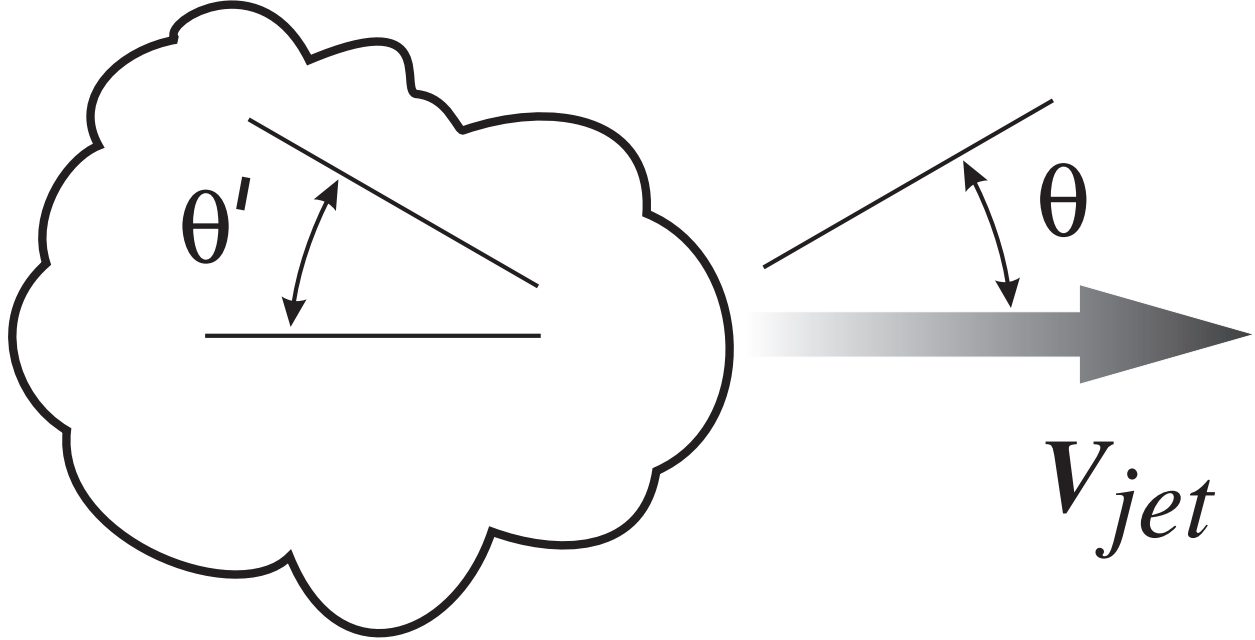


Fig. 1.— Definition of angles in the jet comoving frame (θ') and in the lab frame (θ).

For convenience, let us remind the Lorentz transformations for the quantities to be used in this paper: emission and observation angles (θ' and θ , respectively), frequencies,

and intensities, i.e., energy flux per unit solid angle and per unit frequency. (Prime stands for the jet-frame in the case we need to introduce both the lab-frame and the jet-frame quantities.) The reference frames are defined as shown in Fig. 1; note that the polar axes in the comoving and laboratory frames are directed opposite to each other. Then, we have the following relations

$$\text{for angles: } \cos \theta = \frac{\beta - \cos \theta'}{1 - \beta \cos \theta'} \quad \text{or} \quad \tan \frac{\theta}{2} \tan \frac{\theta'}{2} = \frac{1}{\Gamma(1 + \beta)}, \quad (1)$$

$$\text{for frequencies: } \nu = \Gamma(1 - \beta \cos \theta') \nu' \equiv \delta \nu', \quad (2)$$

$$\text{for intensities: } I(\nu, \theta) = \delta^n I'(\nu', \theta'). \quad (3)$$

Here β is the jet velocity in units of the speed of light c , Γ the jet Lorentz factor, and

$$\delta = \Gamma(1 - \beta \cos \theta') = \frac{1}{\Gamma(1 - \beta \cos \theta)} = \frac{\sin \theta'}{\sin \theta} \quad (4)$$

the Doppler factor. In the last equation, $n = 2$ for a continuous jet and $n = 3$ for a relativistically moving blob (Lind & Blandford 1985). The flux density per unit frequency, F_ν , changes with the observation angle as intensity.

Throughout the paper we will often use the asymptotic form of Eqs. (1), (2) and (3) for the case, where both the observation angle and the emission angle are small ($\theta, \theta' \ll 1$). In terms of observation angle, this condition is equivalent to $\Gamma^{-1} \ll \theta \ll 1$. In this case

$$\delta \simeq \frac{\Gamma \theta'^2}{2} \simeq \frac{2}{\Gamma \theta^2}, \quad \theta \theta' \simeq \frac{2}{\Gamma}. \quad (5)$$

In this paper we consider only uniform jets, i.e., those with Lorentz factor independent on direction and distance from the origin. However, we use this simplification only when considering particular implications in order to present conclusions in a clear form.

The paper is organized as follows. First, we discuss the conditions causing strong off-axis emission from relativistic jets (Sect. 2), then we analyze motion and radiation of particles responsible for this emission (Sect. 3 and 4). After discussing some general results in Sect. 5, we move on to consider implications for particular astrophysical objects (Sect. 6).

2. Conditions for anisotropic emission in the jet frame

Almost in every model of compact objects with relativistic flows the observed radiation comes from particles, which are themselves relativistic in the comoving frame (such a flow is sometimes called a hot jet). Photons produced by a relativistic particle continue to stream

in the direction of the particle’s motion, hence the photon field in the jet frame has the same degree of anisotropy as the particle distribution does. There always exists a continuous anisotropic supply of relativistic particles – those, entering the flow from surrounding medium through the shock front or the shear layer at the jet’s boundary. If their scattering length ℓ_s is shorter than or comparable to their radiation length ℓ_r (both are measured in the jet frame), then the resulting emission can be treated as isotropic. Otherwise, the radiation is essentially anisotropic in the jet frame; in the extreme case it is directed opposite to the velocity of the flow and confined within a narrow cone with the opening angle $\sim \Gamma^{-1}$. Let’s define the critical energy E'_{cr} so that $\ell_s(E'_{\text{cr}}) = \ell_r(E'_{\text{cr}})$. Since ℓ_s/ℓ_r is a monotonically growing function of energy¹, the super-critical particles (those with energies $E > E_{\text{cr}}$) do not get isotropized and produce anisotropic emission.

One can notice that the very nature of diffusive acceleration implies that $\ell_s \lesssim \ell_r$. Indeed, the diffusive acceleration proceeds through multiple passages of an accelerated particle from the jet to surrounding medium and back, and in each round the particle’s energy increases by a factor ~ 2 , even in the case of relativistic shock (e.g., Achterberg et al. 2001). The particle should be able to preserve at least a half of its energy over the scattering length to keep accelerating, so that the condition $\ell_s \lesssim \ell_r$ is automatically satisfied, providing seemingly firm ground to the isotropy assumption.

However, energetic particles emerge in the jet in several other ways as well. They can be accelerated by preceding shocks and survive till the shocked gas slows down to sub-relativistic speeds, or be the secondary electrons from inelastic interactions of higher-energy protons, or be injected in the surrounding medium by the jet itself, as in the case of e^-e^+ -pair loading ahead of GRB shocks (e.g., Madau & Thompson 2000). Also, super-critical particles can be produced via non-diffusive converter acceleration mechanism (Derishev et al. 2003; Stern 2003), in which the energy gain per shock crossing is not limited to the factor ~ 2 . The super-critical particles do not get isotropized by definition, and hence they contribute to the anisotropy of photon field in the jet frame. Although both electrons and protons can be super-critical, the case of electrons is of much larger importance since the acceleration of protons is almost always limited by their diffusive escape of by the accelerator’s lifetime rather than by radiative losses.

It is safe to claim that the emission from relativistic jets is partly contributed by super-critical particles, though how large is this part is the question to be considered separately for various sources. Anyway, smallness of the anisotropic part in the particle distribution

¹The scattering length of a particle in the magnetic field grows linearly proportional to the particle’s energy or faster, whereas the radiation length either decreases or grows no faster than $E/\ln(E)$.

does not mean its contribution to the observed emission is negligible in all spectral domains and at all viewing angles.

3. Motion of super-critical particles and their emission

Suppose that super-critical particles are injected in the jet with highly anisotropic angular distribution, having the opening angle ϕ_0 (in the comoving frame) and elongated counter to the jet's velocity. Over their radiation length, the particles get deflected by an angle ϕ , which is a decreasing function of energy. The characteristic width of the beam pattern in the jet frame (θ_b) equals to that of the particle distribution:

$$\theta'_b(\varepsilon) = \begin{cases} 1 & \text{for } \varepsilon < 1 \\ \phi(\varepsilon) & \text{for } 1 < \varepsilon < \varepsilon_{\text{cr}2} \\ \phi_0 & \text{for } \varepsilon > \varepsilon_{\text{cr}2} . \end{cases} \quad (6)$$

To simplify the notations here and below, we introduce the following dimensionless variables: ε is the particle's energy in units of the critical energy E'_{cr} (so that $\varepsilon_{\text{cr}} \equiv 1$), x the distance in units $\ell_s(E'_{\text{cr}})$, which is the scattering length at the critical energy. The second critical energy $\varepsilon_{\text{cr}2}$ is defined as the energy of particles whose r.m.s. deflection angle equals to the initial width of the particle distribution: $\phi(\varepsilon_{\text{cr}2}) = \phi_0$.

Equation (6) has simple physical meaning. The sub-critical particles ($\varepsilon < 1$) have enough time to get fully isotropized, whereas for super-critical ones the width of the distribution function is equal to their r.m.s. deflection angle ϕ , unless $\phi < \phi_0$. Above the second critical energy $\varepsilon_{\text{cr}2}$, the particles loose energy before being significantly deflected, and the distribution function preserves its intrinsic width ϕ_0 . The latter can be as small as $\phi_0 = \Gamma^{-1}$ (if the distribution is isotropic in the lab frame): for example, the converter acceleration mechanism essentially implies isotropisation of accelerated particles each time when they get into the surrounding medium (Derishev et al. 2003).

Typically, the plasma in relativistic flows is collisionless, i.e., the only scattering mechanism is deflection of charged particles by the magnetic field. For a broad class of the magnetic-field geometries the dependence of the r.m.s. deflection angle on the distance travelled by the particle allows the following representation (for small deflection angles and approximately constant energy):

$$\phi = \frac{x^p}{\varepsilon}. \quad (7)$$

This comprises two widely used limiting cases: small-angle scattering in the purely chaotic magnetic field ($p = 1/2$) and regular deflection in the quasi-uniform magnetic field ($p =$

1), which corresponds to Bohm-like diffusion. Values in the range $1/2 < p < 1$ cover intermediate situations, including scattering in the turbulent magnetic field with power-law power spectrum.

The number of possible energy loss mechanisms, on the other hand, is large. Each of them implies different dependence of the energy loss rate on the particle energy and (in general) on the propagation angle. Moreover, in different energy domains prevalent and negligible mechanisms can swap their roles. To keep the paper reasonably concise, we focus our analysis on three representative cases, marked below by the dominant energy loss channel.

Synchrotron or inverse-Compton (including self-Compton) radiation in the Thomson regime. In this case the energy loss rate is proportional to the square of the particle's energy:

$$\frac{d\varepsilon}{dx} = -\varepsilon^2 \quad \Rightarrow \quad x_r = \frac{1}{\varepsilon}, \quad (8)$$

where x_r is the normalized radiation length. Substituting Eq. (8) into Eq. (7) we find that the beam-pattern width is

$$\theta'_b = \varepsilon^{-(p+1)} \quad (9)$$

for particles in the energy range $1 < \varepsilon < \varepsilon_{\text{cr}2}$.

The typical frequency of emitted photons is $\nu' = \varepsilon^2 \nu'_{\text{cr}}$, and the second critical energy is $\varepsilon_{\text{cr}2} = \phi_0^{-\frac{1}{p+1}}$.

Inverse-Compton radiation in the Klein-Nishina regime. If the spectrum of radiation being comptonized is a power-law, $F'_\nu \propto \nu'^q$, where $-1 < q < 1$, then

$$\frac{d\varepsilon}{dx} = -\varepsilon^{1-q} \quad \Rightarrow \quad x_r = \varepsilon^q. \quad (10)$$

For positive q the radiation length increases with increasing energy, but anyway slower than the scattering length. Thus, substitution of Eq. (10) into Eq. (7) gives the beam-pattern width

$$\theta'_b = \varepsilon^{pq-1}, \quad (11)$$

which exhibits regular (monotonically decreasing) dependence on the particle energy.

The typical frequency of emitted photons is $\nu' = \varepsilon \nu'_{\text{cr}}$, and the second critical energy is $\varepsilon_{\text{cr}2} = \phi_0^{-\frac{1}{1-pq}}$.

Comptonization of external (isotropic in the lab frame) radiation in the Thomson regime. In this case the radiating particles loose their energy through interaction with photons, whose distribution is highly anisotropic in the jet frame. Because of this, the

energy loss rate depends on the particle’s propagation angle, but – for an ultrarelativistic particle – it does not depend on the particular choice of reference frame. Making use of this fact, we calculate the energy loss rate in the lab frame, where it is simply $\dot{E} \propto -E^2$, and find from Eq. (5) that $E \propto \phi^2 \varepsilon$. We get

$$\frac{d\varepsilon}{dx} = -\phi^4 \varepsilon^2 \quad \Rightarrow \quad x_r = \frac{1}{\phi^4 \varepsilon}, \quad (12)$$

where the proportionality coefficient is uniquely defined by the condition $x_r(1) = 1$. Solving Eqs. (7) and (12) for the beam-pattern width gives

$$\theta'_b = \varepsilon^{-\frac{p+1}{4p+1}}. \quad (13)$$

If the external radiation has a logarithmically narrow spectrum, then the typical frequency of emitted photons is $\nu' = \theta'_b^2 \varepsilon^2 \nu'_{\text{cr}} = \varepsilon^{\frac{6p}{4p+1}} \nu'_{\text{cr}}$. The second critical energy is $\varepsilon_{\text{cr2}} = \phi_0^{-\frac{4p+1}{p+1}}$.

The three radiation mechanisms described above give rise to nine qualitatively different situations, depending on what is the main energy loss channel (this determines the beam-pattern width) and what type of emission is observed (this determines the spectral shape). Clearly, the physics of the off-axis emission is still richer due to a possibility of interplay between various radiation mechanisms.

4. Off-axis spectra and luminosity

In what follows, we take a power-law injection of super-critical particles, $|\dot{N}/dE| \propto E^{-s}$ for $E > E_{\text{cr}}$, where $\dot{N}(E) \propto E^{1-s}$ is the injection rate integrated over energies larger than E , and $s > 1$ to keep the number of injected particles finite. In the jet frame, this transforms into the power-law injection with the same index at energies $\varepsilon > 1$ and presumably narrow angular distribution ($\Gamma^{-1} \leq \phi_0 \ll 1$). Generalization for the case of arbitrary injection is straightforward, though cumbersome; we skip it for the sake of brevity.

Because of their large scattering length, the super-critical particles have practically no chance to leave the jet. Instead, they loose energy and form a cooling distribution $dN/d\varepsilon = \dot{N}(\varepsilon)/\dot{\varepsilon}_l$, where $\dot{\varepsilon}_l$ is the total energy loss rate, mainly associated with the dominant radiation mechanism. We also introduce $\dot{\varepsilon}_e$ – the energy loss rate via the mechanism that produces the observed emission. The two can be the same, in which case $\dot{\varepsilon}_l \simeq \dot{\varepsilon}_e$, otherwise $|\dot{\varepsilon}_l| > |\dot{\varepsilon}_e|$.

For a cooling distribution, the angle-averaged spectrum in the comoving frame can be derived in the standard way:

$$\langle F'_\nu(\nu') \rangle \propto \dot{\varepsilon}_e \frac{dN}{d\varepsilon} \left(\frac{d\nu'}{d\varepsilon} \right)^{-1} \propto \frac{\dot{\varepsilon}_e}{\dot{\varepsilon}_l} \nu'^{\frac{2-s-x}{x}}. \quad (14)$$

Here we assumed that emission from each particle is monochromatic with frequency $\nu' \propto \varepsilon^x$ (a caution is necessary with this assumption, as discussed below) and the ratio $\dot{\varepsilon}_e(\varepsilon)/\dot{\varepsilon}_l(\varepsilon)$ is regarded as a function of the frequency, corresponding to emission from particles of energy ε .

The radiation of super-critical particles is concentrated within a narrow cone with opening angle $\theta'_b(\varepsilon)$: outside of this cone the radiation is virtually absent, whereas the apparent flux density within the cone is larger than the angle-averaged one by the factor $4\theta'^{-2}_b$. Thus,

$$F'_\nu(\nu') = \frac{4}{\theta'^2_b} \langle F'_\nu(\nu') \rangle \propto \left(\frac{\dot{\varepsilon}_e}{\theta'^2_b \dot{\varepsilon}_l} \right) \nu'^{\frac{2-s-x}{x}} \quad (15)$$

for $\nu'_{\text{cr}} < \nu' < \nu'_{\text{max}}$, where ν'_{max} is a function of emission angle θ'_b .

Emission observed at an arbitrary angle to the jet axis has two components: the radiation from sub-critical particles, whose spectrum cuts off at ν_{cr} , and is continued to higher frequencies by the radiation from super-critical particles. The true cut-off in the off-axis spectrum at ν_{max} is due to the fact that an observer, looking at a given angle θ to the jet axis, cannot see radiation from energetic particles, whose r.m.s. deflection angle is smaller than $2/(\Gamma\theta)$.

All the changes in the off-axis spectrum as compared to the ordinary head-on emission are entirely due to the factor θ'^{-2}_b , which is a rising function of particles' energy (and hence – of frequency). Therefore, the off-axis spectrum is always harder, and in most cases – much harder, than the head-on spectrum. There is a subtle point in the assumption that each particle emits monochromatic radiation. It works well unless the spectrum given by Eq. (15) is harder than the low-frequency asymptotic in the spectrum of an individual particle. All the hard spectra actually are determined by the low-frequency emission of the most energetic particles and have the corresponding spectral index. Such a spectrum covers the frequency range $\nu'_{\text{cr}} < \nu' < \nu'_{\text{max}}$, extending also below ν'_{cr} up to the point, where it intersects with the (softer) spectrum of sub-critical radiation.

To find the observed luminosity one has to take the appropriate energy loss rates from Eqs. (8), (10), and (12), substitute the beam-pattern width θ'_b in Eq. (15) with the corresponding function of energy and then – energy with frequency, and finally apply the Lorentz transformations given by Eqs. (2) and (3). So, an observer in the lab frame, whose line of

sight makes a small angle $1/\Gamma \ll \theta \ll 1$ with the jet axis, sees the following spectrum:

$$F_\nu(\nu, \theta) \propto \nu^\alpha \quad \text{for} \quad \nu_{\text{cr}} < \nu < \nu_{\text{max}}, \quad (16)$$

where both the critical frequency, $\nu_{\text{cr}} = \delta\nu'_{\text{cr}}$, and the cut-off frequency, $\nu_{\text{max}} = \delta\nu'_{\text{max}}$, are functions of the observation angle. The values of spectral index α , as well as the ratio $\nu_{\text{max}}/\nu_{\text{cr}}$, can be found in Tab. 1, where the summary on the resulting spectra for nine different cases is presented.

Another important aspect of the off-axis emission is the way its appearance changes with the observation angle. It can be characterized by dependence of the cut-off frequency on the viewing angle,

$$\nu_{\text{max}}(\theta) = \delta(\theta)\nu'_{\text{max}}(\theta') = \frac{\nu_{\text{max}}}{\nu_{\text{cr}}} \frac{\delta(\theta)}{\delta(0)} \nu_{\text{cr}}(0) \propto \theta^a, \quad (17)$$

and by the jet luminosity taken at the cut-off, $L_{\text{peak}}(\theta) = \nu_{\text{max}} F_\nu(\nu_{\text{max}}, \theta)$,

$$L_{\text{peak}}(\theta) = \left(\frac{\nu_{\text{max}}}{\nu_{\text{cr}}} \right)^{\alpha+1} \delta^{n+1}(\theta) \nu'_{\text{cr}}(\theta') F'_\nu(\nu'_{\text{cr}}, \theta') = \left(\frac{\nu_{\text{max}}}{\nu_{\text{cr}}} \right)^{\alpha+1} \left(\frac{\delta(\theta)}{\delta(0)} \right)^{n+1} L_{\text{peak}}(0) \propto \theta^b. \quad (18)$$

The values of indices a and b are presented in Tab. 1.

So far, we considered only narrow jets, i.e., those having opening angle smaller than or of the order of Γ^{-1} . For a wide relativistic flow, one needs to integrate over observation angles, which are different for different portions of the flow.

5. Discussion

The off-axis emission is intrinsically high-energy phenomenon. In the case of Bohm diffusion, for instance, the critical energy for electrons, whose acceleration is limited by the synchrotron losses, is

$$E'_{\text{cr}} = \frac{3}{2} \frac{(m_e c^2)^2}{\sqrt{e^3 B'}}, \quad (19)$$

and the associated cut-off frequency of their synchrotron emission is at

$$\nu'_{\text{cr}} \simeq \frac{0.5 e B'}{\pi m_e c} \left(\frac{E'_{\text{cr}}}{m_e c^2} \right)^2, \quad h\nu'_{\text{cr}} \simeq \frac{9}{4} \frac{m_e c^2}{\alpha_f} \simeq 310 m_e c^2, \quad (20)$$

where α_f is the fine structure constant. In the observer's frame the cut-off is blueshifted to GeV range. However, a diffusion faster than the Bohm one results in a smaller cut-off

frequency. For example, in the case of random small-angle scattering

$$h\nu'_{\text{cr}} \simeq \left(\frac{\ell_c}{r_{g0}}\right)^{2/3} \left(\frac{\alpha_f B'}{B_{\text{cr}}}\right)^{1/3} \frac{m_e c^2}{\alpha_f}, \quad (21)$$

where $r_{g0} = m_e c^2/eB'$ is the “cold” gyroradius, ℓ_c the correlation length of the magnetic field, and $B_{\text{cr}} \simeq 4.4 \times 10^{13}$ G. The factor ℓ_c/r_{g0} can be as small as unity (if $\ell_c < r_{g0}$, then electrons radiate in the undulator regime and their cut-off frequency increases with decreasing magnetic-field scale), and inverse Compton losses further decrease the value of ν'_{cr} . In the case of GRBs, where $B' \sim 10^5 - 10^6$ G, we find from Eq. (21) that the cut-off can be located at just few MeV, so that the radiation above the peak in GRB spectra can be interpreted as off-axis synchrotron emission.

An important factor to be kept in mind when considering the off-axis emission is two-photon pair production. Absorption of high-energy photons in this process rapidly makes a source opaque with increase of the viewing angle, effectively limiting its maximum value. There is one particular situation, where interference from the two-photon absorption is always important: it is inverse Compton off-axis emission in the Klein-Nishina regime in the case, where it is the dominant radiation mechanism. Indeed, the off-axis emission implies fast cooling of radiating electrons, i.e., the probability that they interact with target photons is close to unity. The same is true for the comptonized high-energy photons, since the cross-sections for electron-photon and photon-photon interactions are of the same order of magnitude in the Klein-Nishina limit.

As easy to see from Tab. 1, a spectral index of the off-axis emission, as a rule, exceeds -1 . In fact, this is always the case as long as the injection spectrum is hard ($s < 2$). As the injection gets softer, there appear exceptions. The first to break this rule (what happens at any $s > 2$) is IC emission in the Klein-Nishina regime for the case, where it dominates energy losses, the spectrum of comptonized radiation is $F_\nu \propto \nu$, and the magnetic field is quasi-uniform ($p = 1$). The above preconditions, taken together, make this situation rather unlikely. The more common synchrotron emission, on the other hand, is quite resistant in the hardening trend: only very soft injection with $s > 4$ can make its spectral index smaller than -1 . So, in the vast majority of situations, the luminosity at cut-off, L_{peak} , is roughly the same as the bolometric luminosity of the jet.

Since it has many applications, it is interesting to discuss the synchrotron emission in more detail. In the case where it is the dominant radiation mechanism, the spectral index between ν_{cr} and ν_{max} increases by 2 (for the Bohm-like diffusion) or by 1.5 (for random small-angle scattering) relative to what would be the spectral index of ordinary head-on emission. For an injected particle distribution with indices $s < 10/3$ or $s < 7/3$ (the Bohm-like diffusion and the small-angle scattering, respectively), the resulting spectrum formally

appears to be harder than the low-frequency asymptotic for the synchrotron emission of an individual particle. In practice, this means that the spectrum is determined by the low-frequency emission of the most energetic particles. The observed cut-off frequency depends on the viewing angle as $\nu_{\max} \propto \theta^{-1}$ for the Bohm-like diffusion and $\nu_{\max} \propto \theta^{-2/3}$ for the small-angle scattering, that is, much weaker than dictated by the Lorentz transformations alone ($\nu_{\max} \propto \theta^{-2}$).

Prevalence of the external Compton losses reverses the above dependence and even cancels out the effect of jet dimming with increasing viewing angle. Indeed, one finds from Tab. 1 that the cut-off frequency increases with viewing angle as $\nu_{\max} \propto \theta^3$ or $\nu_{\max} \propto \theta^2$ for the Bohm-like diffusion and the small-angle scattering, respectively. Under a widely used assumption that the particle injection function has spectral index $s = 2$, the peak luminosity L_{peak} of a continuous jet appears to be independent on the viewing angle for any p . Moreover, a hard injection with the index $s < 2$ makes an off-axis jet to appear brighter than when it is viewed head-on.

An intermediate situation takes place in the case where self-Compton radiation in the Klein-Nishina regime dominates the energy losses. Here the cut-off frequency may increase or decrease with the viewing angle, depending on whether the spectral index q of the radiation being comptonized is positive or negative.

The off-axis radiation is not necessarily electromagnetic in its nature; for instance, it can be neutrino emission. The only practical source of neutrinos in relativistic jets is the decay of charged pions, which are produced in photo-pionic reactions or in inelastic collisions of nucleons. To be precise, we note that decaying charged pions give muons plus only one half of the total number of muon neutrinos and anti-neutrinos. Another half and all of the electron neutrinos and anti-neutrinos come from subsequent decays of secondary muons. In this way, neutrinos are born alongside with energetic photons, electrons, and positrons, which altogether carry about a half of the energy of decaying pions. This argument apparently leads to the conclusion that the neutrino luminosity of a relativistic jet is at most as large as its electromagnetic luminosity.

Once again, the common wisdom does not work with the off-axis emission. A situation is possible, where the jet is opaque for the high-energy photons, which therefore get reprocessed through electromagnetic cascade, producing isotropic in the jet-comoving frame soft electromagnetic radiation. The latter is strongly beamed in the laboratory frame due to jet's motion. Neutrinos, on the other hand, preserve their initial anisotropy in the comoving frame and can be efficiently emitted at larger angles to the jet axis. When observed at large viewing angles, such a jet looks as an over-efficient neutrino source.

Since the off-axis neutrino emission can originate only from anisotropic angular distribution of the parent pions (muons), it requires substantially anisotropic – in jet frame – source of energetic nucleons. It is possible if acceleration of protons is radiative-loss limited or if there is a neutron component in the jet (Derishev, Kocharyan, & Kocharyan 1999), which moves with the Lorentz factor different from that of the bulk matter. In either case the decay length of pions (muons) must be less than their scattering length not to let them isotropize. In terms of diffusion coefficient $\mathcal{D}(E)$, which depends only on the particle's energy in the ultra-relativistic limit, this condition means

$$\mathcal{D}(E) > \mathcal{D}_i(E) = \frac{1}{3} \frac{t_i}{m_i} E, \quad (22)$$

where the index i stands either for charged pions (π) or muons (μ), $t_\pi \simeq 2.6 \times 10^{-8}$ s and $t_\mu \simeq 2.2 \times 10^{-6}$ s are their lifetimes, m_π and m_μ their masses. If $\mathcal{D}_\pi < \mathcal{D} < \mathcal{D}_\mu$, then only a half of muon neutrinos contribute to the off-axis emission, whereas the beam-pattern for electron neutrinos and the rest of muon ones is similar to that of ordinary emission.

In the case of Bohm diffusion, Eq. (22) translates simply into an upper limit for the magnetic field strength:

$$B < B_i = \frac{m_i c}{e t_i}. \quad (23)$$

Here $B_\pi \simeq 600$ G and $B_\mu \simeq 5$ G, so that the above condition is true for any potential neutrino sources except arguably for the GRB internal shocks, where the diffusion should be orders of magnitude faster than the Bohm diffusion to fulfill Eq. (23).

6. Implications

Many astrophysical sources with relativistic jets change their appearance in presence of the off-axis emission. The difference is negligible at low frequencies, but becomes dramatic for high-energy photons (typically X- and gamma-rays). Unfortunately, it is practically impossible to make definitive and unequivocal predictions from the first principles since the properties of the off-axis emission strongly depend on details of both radiation and acceleration mechanisms, with uncertainties in geometry further increasing the range of possible solutions. The problem, however, has a silver lining from the observational perspective: the very same diversity of unique observational signatures provides a means to determine physical parameters in a source.

In accordance with the above note, this section is not to present a comprehensive analysis of the properties of off-axis emission for various sources, but rather to give an idea of what

one expects in typical situations, that is done below using primarily GRBs as a representative example.

GRBs are a complex phenomenon (see, e.g., [] and [] for a review), which can be decomposed into qualitatively different prompt-emission and afterglow phases. During the prompt phase, which lasts from a fraction of a second to few hundred seconds, GRBs usually have highly irregular lightcurves and relatively hard emission. The afterglow is characterized by gradually decaying smooth lightcurve with occasional rises and regular softening of the emission.

In the following discussion we assume for definiteness that peaks in observed GRB spectra correspond to transition from sub-critical to super-critical radiation regimes, so that the radiation above the peak is mainly due to off-axis emission. Such an interpretation implies that both sub- and super-critical particles form a single distribution. This is possible if the radiating electrons are secondary particles from inelastic interactions of high-energy protons, or produced via a non-diffusive (for example, converter) acceleration mechanism.

The prompt emission of GRBs is thought to be the synchrotron radiation originating from a succession of internal shocks, i.e., those developing within the fireball at a distance of the order of $D \sim 10^{12}$ cm from the central engine. Radiation from a large number of such shocks contributes to observed flux at any moment of time; in effect, they can be treated as a continuous jet. One can imagine two situations: a jet, whose opening angle θ_0 is smaller than the viewing angle θ , and the opposite case of small viewing angle, $\theta < \theta_0$.

The timing properties of the prompt emission are similar in both cases. Since the Doppler factor for off-axis jets is smaller, the variability timescale must be longer. However, the total duration of a burst t_{GRB} is not affected: it is determined by the lifetime of central engine, at least as far as geometrical delay for light propagation is smaller than the lifetime, i.e., $\theta^2 D / 2c \lesssim t_{\text{GRB}}$. Even for short bursts, the latter condition corresponds to relatively large viewing angles $\theta \lesssim 0.1$.

For the case of small viewing angle, observed spectra are affected in two ways. The off-axis emission from edge portions of the jet (those propagating at angles much larger than $1/\Gamma$ to the line of sight) can contribute to: (1) the bolometric luminosity and (2) a high-energy tail above the cut-off frequency. For the synchrotron-self-Compton emission, no matter whether the synchrotron or inverse Compton losses are dominant, the peak luminosity $L_{\text{peak}}(\theta)$ normally ² decreases with increase of the viewing angle faster than θ^{-2} , making the

²The opposite requires either hard injection with $s < 2$ or the low-frequency asymptotic in the spectrum of comptonized radiation harder than $F_\nu \propto \nu^{1/3}$, that is a source of emission other than the synchrotron.

first effect negligible. On the contrary, if the jet loses energy mostly to external Compton radiation, then the edge portions of the jet dominate the overall bolometric luminosity as far as $s < 14/5$, that is, for any reasonable injection. Although prevalence of external Compton losses in the jet’s radiative balance or an injection with the index $s < 2$ are not favored by current GRB theories, we conclude that the edge portions of the jet cannot safely be ignored even when calculating the bolometric luminosity.

If the cut-off frequency ν_{\max} increases with increasing viewing angle, then the off-axis emission from edges of a wide jet significantly changes the observed (composite) spectrum, causing a high-energy tail to appear instead of an exponential cut-off. Parts of the jet viewed at different angles contribute to this tail with luminosities $\propto \theta L_{\text{peak}}(\theta) \propto \theta^{b+1}$, concentrated mostly around frequency $\nu(\theta) \simeq \nu_{\max}(\theta) \propto \theta^a$. The envelope of individual contributions gives the power-law tail:

$$\nu F_{\nu} \propto \nu \left(\theta L_{\text{peak}} \frac{d\theta}{d\nu} \right) \propto \nu^{\frac{2+b}{a}}, \quad (24)$$

where $\theta \propto \nu^{1/a}$ and $a > 0$. As follows from Tab. 1, the condition $a > 0$ can be satisfied in a consistent synchrotron-self-Compton model, for example if comptonization proceeds in the Klein-Nishina regime and the spectral index of comptonized radiation is positive (i.e., $q > 0$), so that emergence of the power-law tail should be considered a common phenomenon.

In the case of large viewing angle, $\theta \gg \theta_0$, every portion of a jet moves at approximately the same angle to the line of sight, so that the situation is in almost every respect equivalent to the case of narrow jet, which was considered in Sect. 4. The only correction to be made is to take into account that the jet subtends an angle, which is much larger than $1/\Gamma$. For an idealized (uniform with sharp edges) jet the corrected dependence of luminosity on the viewing angle is

$$L_{\text{peak}}(\theta) = (\Gamma\theta)^b (\Gamma\theta_0)^2 L_{\text{peak}}(0), \quad (25)$$

where $b < -2$ and $\theta, \theta_0 \gg \Gamma^{-1}$. As the viewing angle exceeds the opening angle of the jet, the bolometric luminosity drops by a factor $\sim (\Gamma\theta_0)^{-2-b}$.

Taking into consideration the off-axis emission, it is interesting to discuss a possibility that the X-ray flashes (XRFs) are normal GRBs, whose jets are not pointing to the observer. The peak energy in XRF spectra is smaller than in GRB spectra, implying that $a < 0$ and, consequently (see Tab. 1), that $b < -3$. Therefore, in the case of idealized jet, the XRFs and GRBs are members of separate source populations, whose average brightness differs by a factor $\Gamma\theta_0 \ll 1$ or smaller. Apart from this difference in brightness, the XRF spectra in their low-energy (below the peak) part should possess the intrinsic feature of off-axis emission – a paucity of soft photons.

Finally, let us discuss of a tempting possibility to explain unusually weak GRBs as off-

axis jet. Unlike XRFs, weak GRBs have luminosities many orders of magnitude smaller than their normal counterparts, but radiate in the same spectral range. The off-axis synchrotron emission can account for the properties of weak GRBs if their main radiative mechanism is self-Compton in the Klein-Nishina regime, and their low-frequency spectral index q is close to zero. Indeed, in this case the cut-off frequency is nearly independent on the viewing angle, whereas the observed luminosity can drop as fast as θ^{-3} .

Unlike the prompt GRB emission, the afterglow comes from a single blast wave, which forms when the GRB ejecta plunge into surrounding interstellar gas and which in most cases can be approximated by a thin spherical shell. Despite the simple geometry, dynamics of this blast wave is complicated by various factors, such as inhomogeneous external medium, formation of multiple sub-shocks, late energy injection, etc., which are beyond the scope of this paper. However, a principal part of the problem – namely, obtaining the Green function for a radiating spherical shell – can be formulated in model-independent terms. Physically, the Green function $G(R, t, \nu)$ is the spectral flux density, measured by a distant observer as a function of time, provided the radiation comes from an instantaneous release of unit energy in a spherical shell of radius R expanding with velocity $v(R)$. By definition, $\int G(R, t, \nu) d\nu dt = 1$ and $G \equiv 0$ for any $t < 0$. The spectrum of any thin blast wave can be represented as

$$F_\nu(t, \nu) = \int_0^\infty \lambda(R) G(R, t - t_e, \nu) dR, \quad (26)$$

where $\lambda(R)$ is the energy lost for radiation per unit distance, and $t_e(R) = \int_0^R \frac{dR}{v(R)} - \frac{R}{c}$ the time, as measured by the distant observer, it takes for the blast wave to expand to the radius R . If necessary, Eq. (26) includes another integration to take into account the radial structure of the blast wave.

To find the Green function, we note that the area of spherical segment that comes into the observer's view during the time interval dt is equal to $2\pi R c dt$. This segment moves at an angle $\theta(t) = \arccos(1 - ct/R)$ to the line of sight and its contribution to the detected fluence is proportional to $\theta^{k(\alpha+1)} \delta^{n+1} dt \propto \delta^{-b/2} dt$, where the index n (see Eq. (3) for definition) is equal to 2. Indeed, physically an element of the blast wave is a blob, whose luminosity scales with $n = 3$, and whose apparent lifetime is proportional to δ^{-1} , so that its fluence scales with $n = 2$. So, we obtain

$$G(R, t, \nu) = \left[\frac{2}{b+2} \frac{R}{\beta c} \left\{ (1 + \beta)^{1+b/2} - (1 - \beta)^{1+b/2} \right\} \right]^{-1} \Theta(t) \Theta \left(\frac{2R}{c} - t \right) \left(1 - \beta + \beta \frac{ct}{R} \right)^{b/2} f(R, \nu, \theta), \quad (27)$$

where $\Theta(t)$ is the step function, $f(R, \nu, \theta)$ the spectral energy distribution, normalized to

unity, and the factor in square brackets ensures that the Green function as a whole is normalized to unity.

Since we are interested in the ultra-relativistic case, where $\beta \rightarrow 1$, it is convenient to use the approximate expression for the Green function,

$$G(R, t, \nu) \simeq \left[-(b+2)\Gamma^2 \frac{c}{R} \right] \Theta(t) \left(1 + 2\Gamma^2 \frac{ct}{R} \right)^{b/2} f(R, \nu, \theta), \quad (28)$$

which is also valid for a blast wave with finite angular extent as long as the opening angle is much larger than Γ^{-1} .

An important thing to learn from Eq. (28) is that a radiating shell fades away rather gradually after the shock has passed it, producing what may be called a geometrical, or retarded, afterglow. Due to the geometrical delay, the retarded emission from early afterglow coexists in time with ordinary emission from late afterglow, and its bolometric luminosity asymptotically decreases as $t^{b/2}$. In absence of the off-axis emission, $b = -6$ and the luminosity of geometrical afterglow rapidly decays to a level, indiscernible against the much brighter ordinary afterglow. For the off-axis emission, the index b is typically in the range $-4 < b < -2$, that corresponds to decay rate of the geometrical afterglow between t^{-2} and t^{-1} . For comparison: the bolometric luminosity of ordinary afterglow behaves as $t^{-3/2}$ and $t^{-12/7}$ for adiabatic and fully radiative shocks, respectively, propagating into uniform medium, or as t^{-1} and $t^{-4/3}$ if the shocks propagate into a wind with density profile $\rho \propto R^{-2}$.

The properties of off-axis emission, which are discussed above in application to GRBs, show up also in AGNs (and microquasars, as far as they can be considered a scaled-down version of AGNs). Thus, we limit our analysis of AGNs to only one specific point – the observational bias against detection of jets pointing away from the line of sight.

With present-day telescopes AGN surveys are sensitivity-limited, i.e., we detect only those, whose apparent brightness is above certain threshold. Let us suppose that the bolometric luminosity changes with the viewing angle as θ^{-b} and the sources are uniformly distributed in space. Then the number of detectable sources decreases with viewing angle as

$$N(\theta) \propto \theta^{\frac{4-3b}{2}}. \quad (29)$$

In absence of the off-axis emission the bolometric luminosity decreases with the viewing angle as θ^{-6} , so that $N(\theta) \propto \theta^{-7}$. Among hundreds of known blazars one can hardly expect to find even a single source with $\theta > 2/\Gamma$, in accordance with the existing observational data. On the other hand, the radiogalaxies are observed with randomly directed jets, that comes at no surprise since the radio-emission is not beamed. The off-axis emission is much less beamed

than the ordinary radiation from AGN inner jets and – in this respect – resembles radio-emission, though it occupies the opposite end of electromagnetic spectrum. The number of detectable off-axis sources increases with increasing index b and they dominate the entire source population for any $b > -4/3$.

It turns out that a situation, typical for blazars (the radiative losses are mostly due to inverse Compton scattering of external photons), provides also an extreme example of the off-axis synchrotron emission, with apparent luminosity almost independent on the viewing angle. It means that the majority of blazars, which are not detected at present because of large inclination of their jets to the line of sight, will show up when observed in the right spectral range. For the synchrotron off-axis emission from MeV blazars the most favorable (from the observational point of view) spectral domain is around 100 MeV, within the operational range of GLAST and AGILE. The inverse Compton component of the off-axis emission can be detected with modern ground-based Cherenkov telescopes, which are sensitive to photons down to 30-100 GeV. Some of these off-axis blazars may have already been detected by EGRET as unidentified high-latitude sources.

7. Conclusions

A number of processes lead to generation of super-critical particles in relativistic flows. Having the scattering length of the order of the radiation length or exceeding it, these particles do not isotropize upon entering the relativistic flow and radiate their energy while preserving a certain degree of anisotropy. This anisotropy counteracts the beaming, which results from the Lorentz boost, so that the emission produced in such a way has a wider beam pattern in the laboratory frame than that of sub-critical particles and can be called the off-axis emission. The properties of the off-axis emission under various conditions are summarized in Table 1. Among many implications considered in this paper, the following are of major importance from the observational point of view.

The jet sources, which are observed off-axis owing to the effect of beam pattern broadening should exhibit very hard spectra. Indeed, for the super-critical particles the r.m.s. deflection angle (and hence the width of the beam pattern) is a function of their energy. An observer situated at a large angle to the jet axis effectively sees the particle distribution devoid of its low-energy part, whose emission can only be seen at smaller viewing angles. Therefore, the off-axis emission is the hardest possible – in most cases it is essentially as hard as the spectrum of an individual particle. An off-axis jet (for example, AGN, GRB, or microquasar) is likely to be a source of gamma-ray radiation above several MeV and up to TeV range without any bright X-ray or optical counterpart. Apparently, the off-axis AGNs

can account at least for some of unidentified extragalactic EGRET sources.

The space-borne gamma-ray telescopes with wide field of view, such as GLAST and AGILE, have the greatest chance to detect synchrotron radiation from off-axis jets. The inverse Compton component of the off-axis emission can be detected by ground-based Cherenkov telescopes. However, they have very limited surveying capabilities, so that the best observing strategy in search of the off-axis emission would be to look at known AGNs whose jet are pointing away from the line of sight.

In transient sources (for example, GRBs) broader beam pattern means larger geometrical delay, which is proportional to the square of angle between the jet axis and the line of sight. The luminosity of in the retarded off-axis emission decays rather slowly in time, allowing observations in GeV-TeV range when the prompt emission is over. Moreover, if the temporal index of geometrical afterglow is larger than $-3/2$ (that is right in the middle of the typical range), then the integral signal-to-noise ratio continually grows with observing time as long as the off-axis emission is present. This opens an interesting possibility for observation of GRBs with ground-based Cherenkov telescopes, which normally have to slow response to catch the prompt radiation. A serendipitous discovery of orphan GRB afterglows in the TeV range is also possible, because the beam pattern is broader for high-energy photons. It should be noted that there is observational evidence for delayed GRB emission, at least in the case of GRB940217 (Hurley et al., 1994), which can be interpreted as geometrical afterglow due to the off-axis emission.

The off-axis emission is intrinsically high-energy phenomenon and in some cases it may experience two-photon absorption within the source, especially at large viewing angles. In opaque sources the electromagnetic radiation from super-critical particles is reprocessed through the electromagnetic cascade, loses its identity and becomes collimated, but the neutrino signal from them still comes out. Such jets, when viewed off-axis, appear over-efficient neutrino sources, where the ratio of neutrino luminosity to the electromagnetic one can be almost arbitrarily large. The off-axis neutrinos can be detected by the next generation of cubic-kilometer scale high-energy neutrino detectors, and may provide unique information on the details and relative importance of various particle acceleration processes.

8. Acknowledgments

E.V. Derishev acknowledges the support from the President of the Russian Federation Program for Support of Young Scientists (grant no. MK-2752.2005.2). This work was also supported by the RFBR grants no. 05-02-17525 and 04-02-16987, the President of

the Russian Federation Program for Support of Leading Scientific Schools (grant no. NSh-4588.2006.2), and the program ”Origin and Evolution of Stars and Galaxies” of the Presidium of the Russian Academy of Science.

REFERENCES

Achterberg, A., Gallant, Y.A., Kirk, J.G., Guthmann, A.W. 2001, MNRAS, 328, 393

Derishev, E.V., Kocharovsky, V.V., & Kocharovsky, Vl. V. 1999, ApJ, 521, 640

Derishev, E.V., Aharonian, F.A., Kocharovsky, V.V., Kocharovsky, Vl.V. 2003, Phys. Rev. D, 68, 043003

Hurley, K. et al. 1994, Nature, 372, 652

Lind, K.R., & Blandford, R.D. 1985, ApJ, 295, 358

Madau, P., & Thompson, C. 2000, ApJ, 534, 239

Piran, T. 2005, Rev. Mod. Phys., 76, 1143

Stern, B.E. 2003, MNRAS, 352, L35

Urry, C.M., & Padovani, P. 1995, PASP, 107, 803

Zhang, B., & Mészáros, P. 2004, IJMPA, 19, 2385

Observed emission	Dominant energy loss mechanism		
	Synchrotron or IC	IC in the KN Regime	External Compton
Synchrotron or IC	$\alpha = p + 1 - \frac{s}{2}$ $k = \frac{2}{p + 1}$ $a = -\frac{2p}{p + 1}$ $b = \frac{2}{p + 1} - \frac{s}{p + 1} - 2n$	$\alpha = \frac{3}{2} - \left(p - \frac{1}{2}\right)q - \frac{s}{2}$ $k = \frac{2}{1 - pq}$ $a = \frac{2pq}{1 - pq}$ $b = \frac{3 + q - s}{1 - pq} - 2n$	$\alpha = \frac{3(p + 1)}{4p + 1} - \frac{s}{2}$ $k = 2 + \frac{6p}{p + 1}$ $a = \frac{6p}{p + 1}$ $b = \frac{6(2p + 1)}{p + 1} - \frac{4p + 1}{p + 1}s - 2n$
IC in the KN Regime	$\alpha = 2(p + 1) - q - s$ $k = \frac{1}{p + 1}$ $a = -\frac{2p + 1}{p + 1}$ $b = \frac{1 - q - s}{p + 1} - 2n$	$\alpha = 3 - 2pq - s$ $k = \frac{1}{1 - pq}$ $a = \frac{2pq - 1}{1 - pq}$ $b = \frac{2 - s}{1 - pq} - 2n$	$\alpha = \frac{6(p + 1)}{4p + 1} - q - s$ $k = 1 + \frac{3p}{p + 1}$ $a = \frac{3p}{p + 1} - 1$ $b = \frac{3p}{p + 1} - \frac{4p + 1}{p + 1}(q + s) + 5 - 2n$
External Compton	$\alpha = \frac{4}{3}(p + 1) - \frac{4p + 1}{6p}s$ $k = \frac{6p}{(p + 1)(4p + 1)}$ $a = -\frac{2p}{p + 1} - \frac{2}{4p + 1}$ $b = \frac{4p - 2}{(p + 1)(4p + 1)} - \frac{s}{p + 1} - 2n$	$\alpha = \frac{4p + 1}{6p}(3 + q - 2pq - s) - \frac{p + 1}{3p}$ $k = \frac{6p}{(1 - pq)(4p + 1)}$ $a = \frac{6p}{(1 - pq)(4p + 1)} - 2$ $b = \frac{4p - 2}{(1 - pq)(4p + 1)} + \frac{1 + q - s}{1 - pq} - 2n$	$\alpha = \frac{2(p + 1)}{3p} - \frac{4p + 1}{6p}s$ $k = \frac{6p}{p + 1}$ $a = \frac{4p - 2}{p + 1}$ $b = \frac{4p + 1}{p + 1}(2 - s) - 2n$

Table 1: The summary on indices, which describe the spectrum of off-axis emission, $F_\nu \propto \nu^\alpha$, and its extent in frequency, $\nu_{\max}/\nu_{\text{cr}} = (\Gamma\theta/2)^k$. The table also presents the angular dependence of the cut-off frequency and luminosity at the peak, $\nu_{\max} \propto \theta^a$ and $L_{\text{peak}} \propto \theta^b$, respectively. The viewing angle is in the range $\Gamma^{-1} \ll \theta \ll 1$. For the details on evaluation of these indices see text.